Journal of Mathematical Modeling
Vol. 6, No. 2, 2018, pp. 149-164

JMM

A mathematical modeling of pulsatile blood flow through a stenosed artery under effect of a magnetic field

Ahmad Reza Haghighi[†*] **and Nooshin Aliashrafi**[‡]

[†] *Technical and Vocational University, Tehran, Iran*
[‡] *Urmia University of Technology, Urmia, Iran*
emails: ah.haghighi@uut.ac.ir, naliashrafi@yahoo.com

Abstract. A mathematical model for two-dimensional pulsatile blood flow through a constriction vessels under magnetic field and body acceleration is numerically simulated. The artery considered as an elastic cylindrical tube and the geometry of the constriction assumed to time-dependent with an aim to provide resemblance to the in-vivo situations. The blood flow considered nonlinear, incompressible and fully developed. The nonlinear momentum and the continuity equations under suitable initial and boundary conditions can be numerically solved using the Crank-Nicolson scheme. The blood flow specifications such as the velocity profile, the volumetric flow rate and the resistance to flow are obtained and effects of the magnetic field and the severity of the stenosis under these flow specifications are discussed. Besides the blood flow characteristics through elastic artery have been compared with the rigid ones.

Keywords: Blood flow, Magnetic field, Body acceleration, Crank-Nicolson scheme
AMS Subject Classification: 92B05, 92A08.

1 Introduction

The main reason of death in many countries is Cardiovascular illness [20]. Muliple plaques formation and accumulation of fatty materials such as

[*]Corresponding author.
Received: 12 Dec 2017 / Revised: 12 May 2018 / Accepted: 30 May 2018.
DOI: 10.22124/jmm.2018.9259.1137

cholesterol and triglyceride in the blood vessel lumen can cause cardiovascular diseases. Plaques deposits lead the internal surface of the blood arteries to become irregular and the lumen to become narrow, and may cause a severe reduction in blood flow. If the blood clot develops in coronary arteries, the risk of myocardial infarct would be increased and leads to stroke in the vessels supplying blood to brain.

Blood is a suspension of erythrocytes, white blood cellules, leukocytes, and platelets in a fluid called plasma [16, 25, 33]. Erythrocytes in terms of the number in ratio of other blood suspended cells are in the majority, and their properties are dominant for other cells [24]. Ponalagusmy and Selvi have developed a mathematical model for blood flow through arterial stenosis with the two-fluid model, consisting of a core region of Casson fluid and a circumferential layer of the Newtonian fluid. They concluded that the downstream of the stenotic regions is more important for the diagnosis of vessel illnesses [23]. Haghighi et al. have studied the two-dimensional, pulsatile and two-layered flow of blood through a tapered exible artery [5] and also, in their another research, they solved the governing equations by using the finite difference method and examined the effect of different factors such as the artery tapering, the presence of stenosis and the wall motion on blood flow specifications [9].

The flow of blood under the influence of body acceleration is significantly affected, while driving a vehicle or flying in an aircraft, because the blood flow in vibration environment, and due to which there may occur serious health problems such as loss of vision, headache, increase of pulse rate and hemorrhage in face, neck and brain. Sankar and Lee have studied the pulsatile flow of blood among an arterial stenosis with considering blood as a core region of Casson fluid and a peripheral layer of Newtonian fluid under the body acceleration [27]. Also Shit and Roy examined the pulsatile flow of blood among a stenosed vessel under the periodic body acceleration and then analyzed the heat transfer phenomena by constant blood viscosity [29].

Marques et al. have investigated the pulsatile blood flow in a human vessel that the artery is supposed as being a straight wall tube, and the blood flow is considered to be incompressible and axisymmetric. As well as, the result of pulsatile flow is considered into account with imposing the velocity of the cardiac cycle [14]. Chakravarty and Mandal take blood flow as non-linear and incompressible through stenosed artery and investigated the blood flow characteristics. They noted that assumption of rigid vessels is not acceptable, so the vessels are assumed to be elastic and the geometry of the stenosis considered as time-dependent [3].

The magnetic field has an enormous application as controlling blood flow during surgery. In this field, Misra et al. have studied different kids of flow behavior of blood in arteries by treating non Newtonian and Newtonian fluid under the magnetic field [17–19]. Mekheimer et al. have investigated a mathematical model for flow of blood among an elastic vessel having many stenosis in the presence of magnetic field and also they noted that the mechanical attributes of the vascular wall together with the flow of blood specifications [15]. Shit has developed a computational model for flow of blood under the magnetic field that in this model he reported that no clinical disorders are seen for human health when exposed to a magnetic field of strength up to 9T. [30]. Allshare et al. have examined the steady flow of blood simulations in an axisymmetric vessel stenosis with treating non Newtonian fluid model under the magnetic field. They analyzed the shear thinning behavior of blood [1].

In this paper, the reason to pulsatile pressure gradient arising from systematic functioning of the heart, the blood flow has been assumed unsteady. Haghighi and Asl, solved the pulsatile and two-dimensional blood flow among a tapered artery with overlapping stenosis by using a finite difference method and showed that affects the blood of flow characteristics [6]. The aim of this investigation is assumed the blood flow under the magnetic field and body acceleration. The governing equations which are nondimensional and their boundary and initial conditions are prescribed then solved using finite difference Crank-Nicolson method. The aim of this research is analyze the effect of several factors such as the magnetic field, the presence of stenosis and heat transfer and body acceleration on flow of blood characteristics.

2 Mathematical formulation and analysis

2.1 The geometry of the stenosis

Let us consider a two-dimensional, laminar, unsteady, fully developed and axially symmetric blood flow through a stenosed artery. Let (r, θ, z) be the coordinates of a material point in the cylindrical polar coordinates system in which z is taken along the axial direction respectively and r, θ are taken along the radial and circumferential directions. The geometry of the time variant stenosis is constructed mathematically as: (see Figure 1) [7, 26, 32].

$$R(z,t) = \begin{cases} 1 - A[l_0^{n-1}(z-d) - (z-d)^n]a_1(t), & d \leq z \leq d + l_0, \\ a_1(t), & otherwise, \end{cases} \tag{1}$$

where $A = \frac{\delta}{R_0 L_0^n} \frac{n^{n(n-1)}}{(n-1)}$, $R(z,t)$ is the radius of the arterial segment in the constricted region, R_0 is the radius of the nonstenotic artery, L is the finite length of the arterial segment, l_0 is the length of the stenosis, d is the upstream length of the artery and τ_m is the critical height of the stenosis. $n \geq 2$ is the parameter representing the asymmetry of the stenosis, where $n = 2$ represents that the stenosis is symmetric. The time variant parameter $a_1(t)$ is given by $a_1(t) = 1 + k_r \cos(wt + \varphi)$, in which k_r represents the amplitude parameter and φ is the phase angle.

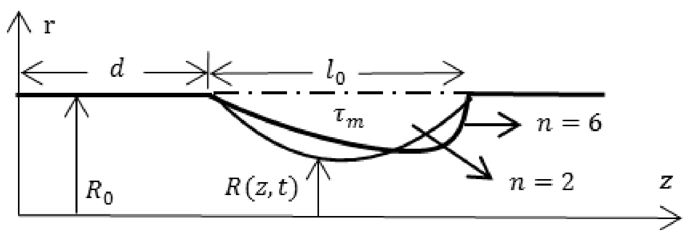

Figure 1: Geometry of the stenosed artery.

2.2 Governing equations

The Navier-Stokes equations for the blood flow in the cylindrical coordinates system (r, θ, z) may be written in non-dimensional forms as follows [4, 6, 11, 12, 17, 31]:
Equation of continuity:

$$\frac{\partial u}{\partial z} + \frac{\partial v}{\partial r} + \frac{v}{r} = 0. \tag{2}$$

Equation of axial momentum:

$$\frac{\partial u}{\partial t} + v\frac{\partial u}{\partial r} + u\frac{\partial u}{\partial z} = -\frac{\partial p}{\partial z} + \frac{1}{\alpha^2}\left(\frac{\partial^2 u}{\partial r^2} + \frac{1}{r}\frac{\partial u}{\partial r} + \frac{\partial^2 u}{\partial z^2}\right) - \frac{1}{\alpha^2}(h)^2 u + \frac{1}{\alpha^2} G(t). \tag{3}$$

Equation of radial momentum:

$$\frac{\partial v}{\partial t} + v\frac{\partial v}{\partial r} + u\frac{\partial v}{\partial z} = -\frac{\partial p}{\partial r} + \frac{1}{\alpha^2}\left(\frac{\partial^2 v}{\partial r^2} + \frac{1}{r}\frac{\partial v}{\partial r} + \frac{\partial^2 v}{\partial z^2} - \frac{v}{r^2}\right). \tag{4}$$

The nondimensional variables that are used in Eqs. (2)-(4) are as:

$$u = \frac{u^*}{U}, \quad v = \frac{v^*}{U}, \quad r = \frac{r^*}{R_0}, \quad l_0 = \frac{l_0^*}{R_0}, \quad z = \frac{z^*}{R_0}, \quad t = \frac{t^* U}{R_0},$$

$$d = \frac{d^*}{R_0}, \quad p = \frac{p^*}{\rho U^2}, \quad Re = \frac{\rho U R_0}{\mu}.$$

which u and v are the axial and the radial dimensionless velocity components, respectively, p is the pressure, ρ is the density and μ is the viscosity.

In the above equations, the other dimensionless variables are taken as follows [31]:

$$\alpha^2 = \frac{U R_0}{\nu}, \quad h = B_0 R_0 \sqrt{\frac{\sigma}{\rho \nu}},$$

where α^2 is the Womersley parameter and h is the Hartmann number.

The dimensionless pressure gradient $\frac{\partial p}{\partial z}$ appearing in Eqs. (2)-(4) is given by: $-\frac{\partial p}{\partial z} = A_0 + A_1 \cos \omega t, \quad t > 0$ [8] where A_0 is the constant amplitude of the pressure gradient, A_1 is the amplitude of the pulsatile component giving rise to the systolic and diastolic pressures and $w = 2\pi f_p$, f_p is the pulse frequency. Using the non-dimensional quantities $a_0 = \frac{R_0^2 a_0^*}{\nu U}$ and $b = \frac{w_b}{w}$ the body acceleration expression defined in the following form [31]:

$$G(t) = a_0 \cos(bt + \varphi_g). \tag{5}$$

The initial and boundary conditions are taken as [11]:

$$r = 0: \quad v(r,z,t) = 0, \quad \frac{\partial u(r,z,t)}{\partial r} = 0, \tag{6}$$

$$r = R(z): \quad v(r,z,t) = \frac{\partial R}{\partial t}, \quad u(r,z,t) = 0, \tag{7}$$

$$v(r,z,0) = u(r,z,0) = 0. \tag{8}$$

2.3 The radial coordinate transformation

The radial coordinate transformation given by $\xi = \frac{r}{R}$ [2,4,11,13,21,22,28], is introduced to transform stenosed artery to straight artery. Using this transformation, Eqs. (2)-(4) and prescribed boundary conditions take the following forms:

$$\frac{\partial u}{\partial t} = -\frac{\partial p}{\partial z} + \frac{1}{R}\frac{\partial u}{\partial \xi}\left[\xi\left(u\frac{\partial R}{\partial z} + \frac{\partial R}{\partial t}\right) - v\right] - u\frac{\partial u}{\partial z}$$
$$+ \frac{1}{\alpha^2}\left[\frac{1}{R^2}\left\{1 + (\xi\frac{\partial R}{\partial z})^2\right\}\frac{\partial^2 u}{\partial \xi^2} + \frac{1}{\xi R^2}\left\{1 + 2(\xi\frac{\partial R}{\partial z})^2\right.\right.$$
$$\left.\left. - \xi^2 R\frac{\partial^2 R}{\partial z^2}\right\}\frac{\partial u}{\partial \xi} + \frac{\partial^2 u}{\partial z^2}\right] - \frac{1}{\alpha^2}(h)^2 u + \frac{1}{\alpha^2}G(t), \tag{9}$$

$$\frac{1}{R}\frac{\partial v}{\partial \xi}+\frac{v}{\xi R}+\frac{\partial u}{\partial z}-\frac{\xi}{R}\frac{\partial R}{\partial z}\frac{\partial u}{\partial \xi}=0, \tag{10}$$

$$\xi=0: \quad v(\xi,z,t)=0, \quad \frac{\partial u(\xi,z,t)}{\partial \xi}=0, \tag{11}$$

$$\xi=1: \quad v(\xi,z,t)=\frac{\partial R}{\partial t}, \quad u(\xi,z,t)=0, \tag{12}$$

$$u(\xi,z,0)=v(\xi,z,0)=0. \tag{13}$$

3 The velocity profile

3.1 The radial velocity component

Multiplying Eq. (10) by ξR and integrating with respect to ξ from 0 to ξ, one can obtain:

$$\xi v(\xi,z,t)+R\int_0^{\xi}\xi\frac{\partial u}{\partial z}d\xi-\frac{\partial R}{\partial z}\xi^2 u+\frac{\partial R}{\partial z}\int_0^{\xi}2\xi u d\xi=0, \tag{14}$$

$$v(\xi,z,t)=-\frac{R}{\xi}\int_0^{\xi}\xi\frac{\partial u}{\partial z}d\xi+\frac{\partial R}{\partial z}(\xi u-\frac{2}{\xi}\int_0^{\xi}\xi u d\xi). \tag{15}$$

For $\xi=1$, by using the boundary conditions (12), Eq. (15) becomes:

$$\int_0^1\xi\frac{\partial u}{\partial z}d\xi=-\int_0^1\frac{2}{R}\frac{\partial R}{\partial z}\xi u d\xi+\int_0^1\frac{1}{R}(\frac{\partial R}{\partial t}\xi f(\xi))d\xi, \tag{16}$$

in which $f(\xi)$ represents an arbitrary function satisfying $\int_0^{\xi}\xi f(\xi)d\xi=1$. Let $f(\xi)=-4(1-\xi^2)$, then from Eq. (15) one can obtain

$$\frac{\partial u}{\partial z}=-\frac{2}{R}\frac{\partial R}{\partial z}u-\frac{4}{R}(1-\xi^2)\frac{\partial R}{\partial t}. \tag{17}$$

By substituting (17) into (15), the radial velocity component may be written as follows:

$$v(\xi,z,t)=\xi[\frac{\partial R}{\partial z}u+\frac{\partial R}{\partial t}(2-\xi^2)]. \tag{18}$$

3.2 The axial velocity component

The Crank-Nicolson scheme for solving Eq. (9) is based upon the central difference formula for all spatial derivatives and the forward difference formula for all time derivative as follows:

$$\frac{\partial u}{\partial \xi}=\frac{1}{2}[\frac{(u)_{i,j+1}^{k}-(u)_{i,j-1}^{k}}{2\Delta\xi}+\frac{(u)_{i,j+1}^{k+1}-(u)_{i,j-1}^{k+1}}{2\Delta\xi}], \tag{19}$$

$$\frac{\partial u}{\partial z} = \frac{(u)^k_{i+1,j} - (u)^k_{i-1,j}}{2\Delta z}, \tag{20}$$

$$\frac{\partial^2 u}{\partial \xi^2} = \frac{1}{2}[\frac{(u)^k_{i,j+1} - 2(u)^k_{i,j} + (u)^k_{i,j-1}}{\Delta \xi^2} + \frac{(u)^{k+1}_{i,j+1} - 2(u)^{k+1}_{i,j} + (u)^{k+1}_{i,j-1}}{\Delta \xi^2}], \tag{21}$$

$$\frac{\partial^2 u}{\partial z^2} = \frac{(u)^k_{i+1,j} - 2(u)^k_{i,j} + (u)^k_{i-1,j}}{\Delta z^2}, \tag{22}$$

$$\frac{\partial u}{\partial t} = \frac{(u)^{k+1}_{i,j} - (u)^k_{i,j}}{\Delta t}. \tag{23}$$

In the above we define:

$$\xi_j = (j-1)\Delta\xi, \quad (j = 1, 2, \ldots, N+1); \quad \xi_{(N+1)} = 1,$$
$$z_i = (i-1)\Delta z, \quad (i = 1, 2, \ldots, M+1),$$
$$t_k = (k-1)\Delta t, \quad (k = 1, 2, \ldots),$$

where $\Delta\xi$, Δz are increment in the radial and the axial directions respectively and Δt is the small time increment.

Using the Crank-Nicolson scheme, the discretized form of Eq. (9) is given as:

$$A_{i,j} u^{k+1}_{i,j-1} + B_{i,j} u^{k+1}_{i,j} + C_{i,j} u^{k+1}_{i,j+1} = D_{i,j}. \tag{24}$$

where

$$A_{i,j} = \frac{\Delta t}{4R^k_i \Delta\xi}[\xi_j(u_{i,j}(\frac{\partial R}{\partial z})^k_i + (\frac{\partial R}{\partial t})^k_i) - v_{i,j}] - \frac{\Delta t}{2\alpha^2 (R^k_i)^2 \Delta\xi^2}\{1 + (\xi_j(\frac{\partial R}{\partial z})^k_i)^2\}$$
$$+ \frac{\Delta t}{4\alpha^2 (R^k_i)^2 \xi_j \Delta\xi}\{1 + 2(\xi_j(\frac{\partial R}{\partial z})^k_i)^2 - \xi_j^2 R^k_i (\frac{\partial^2 R}{\partial z^2})^k_i\},$$

$$B_{i,j} = 1 + \frac{\Delta t}{\alpha^2 (R^k_i)^2 \Delta\xi^2}\{1 + (\xi_j(\frac{\partial R}{\partial z})^k_i)^2\},$$

$$C_{i,j} = \frac{-\Delta t}{4R^k_i \Delta\xi}[\xi_j(u_{i,j}(\frac{\partial R}{\partial z})^k_i + (\frac{\partial R}{\partial t})^k_i) - v_{i,j}] - \frac{\Delta t}{2\alpha^2 (R^k_i)^2 \Delta\xi^2}\{1 + (\xi_j(\frac{\partial R}{\partial z})^k_i)^2\}$$
$$- \frac{\Delta t}{2\alpha^2 (R^k_i)^2 \xi_j \Delta\xi}\{1 + 2(\xi_j(\frac{\partial R}{\partial z})^k_i)^2 - \xi_j^2 R^k_j (\frac{\partial^2 R}{\partial z^2})^k_i\},$$

$$D_{i,j} = u^k_{i,j} - \Delta t(\frac{\partial R}{\partial z}) + \frac{\Delta t}{4R^k_i \Delta\xi}((u)^k_{i,j+1} - (u)^k_{i,j-1})[\xi_j(u_{i,j}(\frac{\partial R}{\partial z})^k_i + (\frac{\partial R}{\partial t})^k_i) - v_{i,j}]$$

$$-\frac{\Delta t}{2\Delta z}(u)^k_{i,j}((u)^k_{i+1,j}-(u)^k_{i-1,j})+\frac{\Delta t}{2\alpha^2(R^k_i)^2\Delta\xi^2}((u)^k_{i,j+1}-2(u)^k_{i,j}$$
$$+(u)^k_{i,j-1})\{1+(\xi_j(\frac{\partial R}{\partial z})^k_i)^2\}+\frac{\Delta t}{4\alpha^2(R^k_i)^2\xi_j\Delta\xi^2}\{1+2(\xi_j(\frac{\partial R}{\partial z})^k_i)^2$$
$$-\xi_j^2R^k_i(\frac{\partial^2 R}{\partial z^2})^k_i\}((u)^k_{i,j+1}-(u)^k_{i,j-1})+\frac{\Delta t}{\alpha^2\Delta z^2}((u)^k_{i+1,j}-2(u)^k_{i,j}$$
$$+(u)^k_{i-1,j})+\Delta t(\frac{G(t)}{\alpha^2})-\Delta t(\frac{h^2}{\alpha^2})u_{i,j}.$$

After computing the velocity distribution, one can compute the volumetric floe rate (Q) and the resistive impedance (Λ) by using the following formulas:

$$Q^k_i=2\pi(R^k_i)^2\int_0^1\xi_j(u)^k_{i,j}d\xi_j,$$
$$\Lambda^k_i=\frac{\left|L(\frac{\partial p}{\partial z})^k_i\right|}{Q^k_i}. \tag{25}$$

4 Numerical Results and Discussion

Numerical computations are performed using the underneath data values [3, 11, 22]:

$$\Delta t=0.001,\quad \Delta\xi=0.0125,\quad \Delta z=0.1,\quad d=10,\quad \alpha=4,\quad f_p=1.2,$$
$$L=30,\quad l_0=14,\quad A_0=0.1,\quad A_1=0.2A_0,\quad R_0=1.52,$$
$$k_r=0.05,\quad a_0=1,\quad \varphi_g=\frac{\pi}{4},\quad \varphi=0,\quad b=1.$$

In order to validate the proposed results, the obtained axial velocity in maximum constricted region for $\tau_m=0.2R_0$ and at the time $t=2$ is compared with the corresponding results obtained by Shaw et al. [28] and Mandal et al. [13].

Figure 3 illustrates the dimensionless axial velocity of the flowing blood at a specific location of $z=17$ in the stenotic region at $t=2$ and $n=2$, $\tau_m=0.2R_0$ for several amount of Hartmann number. In this figure, the axial velocity reduces with decreasing the Hartmann number. This occurs due to the interaction of magnetic field by blood flow, and also a body force per unit volume, known as the Lorentz force, which has a tendency to slow down the motion of fluid, and the axial velocity occurs maximum at the central line of the artery in all four cases.

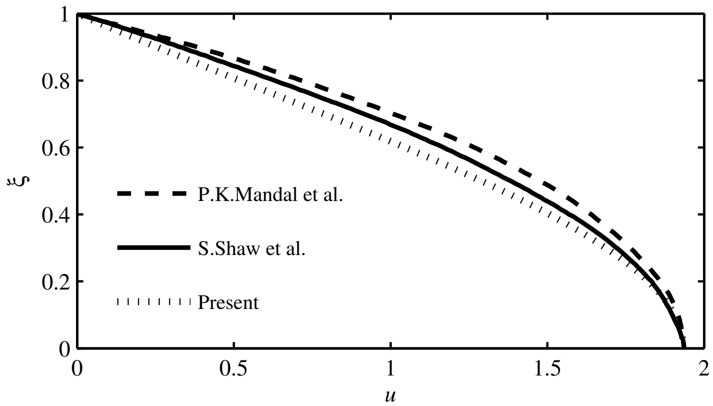

Figure 2: Comparison of the dimensionless axial velocity profile.

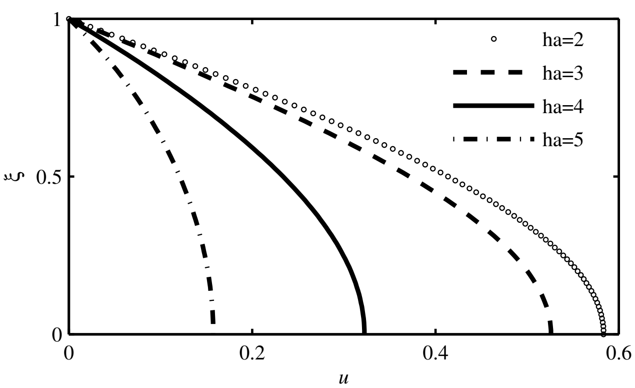

Figure 3: Dimensionless axial velocity profile for different values of Hartmann number.

Figure 4 shows the dimensionless axial velocity profiles for different stenosis sizes at $h = 2$ and $n = 2$. Figure 4 depicted that the axial velocity reduces with increasing the size of stenosis, at $t = 3$. The present figure also consists the axial velocity at the time $t = 2$ among an elastic and rigid artery that the axial velocity in rigid artery is more than the axial velocity in elastic artery and this displays the importance of the assumption of elastic nature of blood vessels.

The rate of flow in the stenosed artery for different Hartmann number at the time $t = 2$, $n = 2$ and $\tau_m = 0.2R_0$ is shown in Figure 5. It is seen that the rate of flow reduces by the increase of the Hartmann number. As a consequence, under the action of a magnetic field, the volume of blood

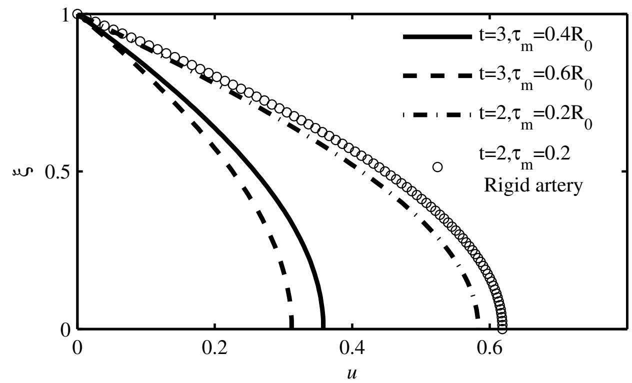

Figure 4: Dimensionless axial velocity profile for different stenosis size.

flow may be adjusted during surgeries.

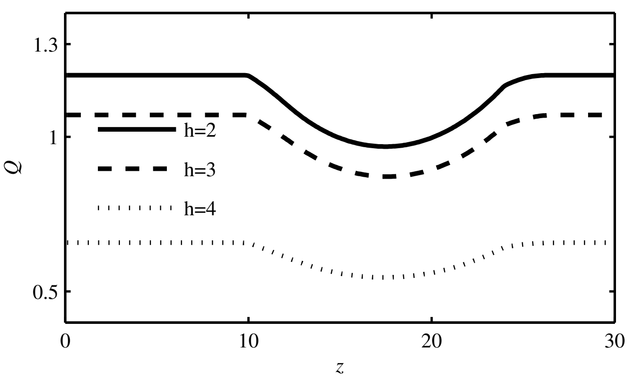

Figure 5: Distribution of the rate of flow for different values of Hartmann number.

Figure 6 shows the comparison results of the rate of flow in the flowing of blood through an elastic and rigid artery together with the evaluation of the effect of the stenosis size on the rate of flow. As shown in figure, the flow rate among the elastic artery at the time $t = 2$, $h = 2$ and $n = 2$ is less than the flow rate through the rigid artery. Also, the rate of flow reduces by the increase at the stenosis size. It is seen that the rate of flow behavior is corresponding to the geometry of the stenosis so that, at the onset of the stenosis rate of flow dropped and at the stenosis critical height reaches to its lowermost level.

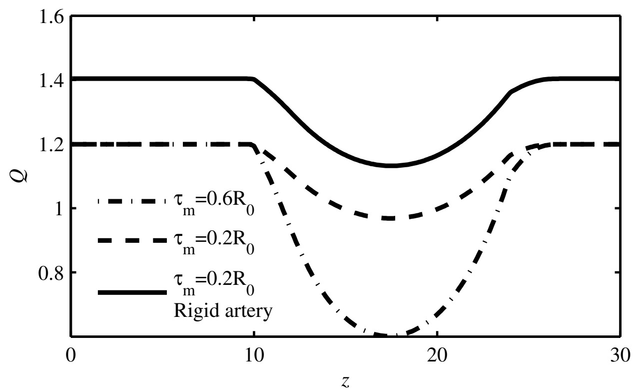

Figure 6: Distribution of the rate of flow for different stenosis size.

Figure 7 describes the three dimensional rate of flow along time t and the axial direction z. It demonstrates that the rate of flow increases with the decreases of the time.

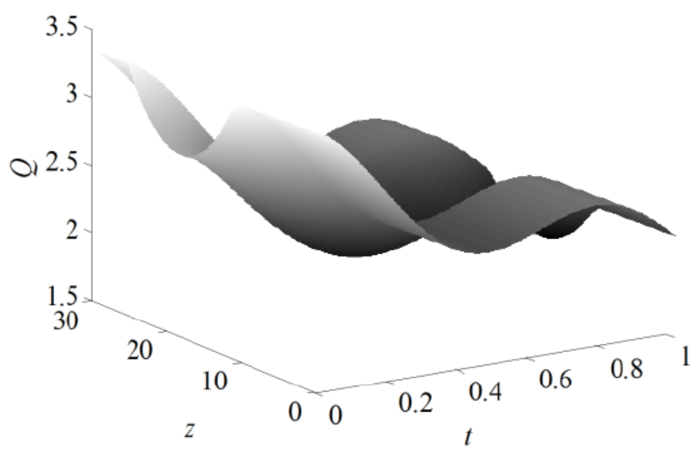

Figure 7: Surface plot of the volumetric flow rate

Resistive impedance through a stenosed artery for different Hartmann number at the time $t = 2$, $n = 2$ and $\tau_m = 0.2R_0$ is presented in Figure 8. Considering Eq. (25) the rate of flow and the resistive impedance are inversely relevant, thus unlike the rate of flow, the resistive impedance increases by the increase in the Hartmann number.

The resistive impedance in the stenosed vessel for several stenosis sizes at the time $t = 2$, $n = 2$ and $h = 2$ is obvious in Figure 9. It has been

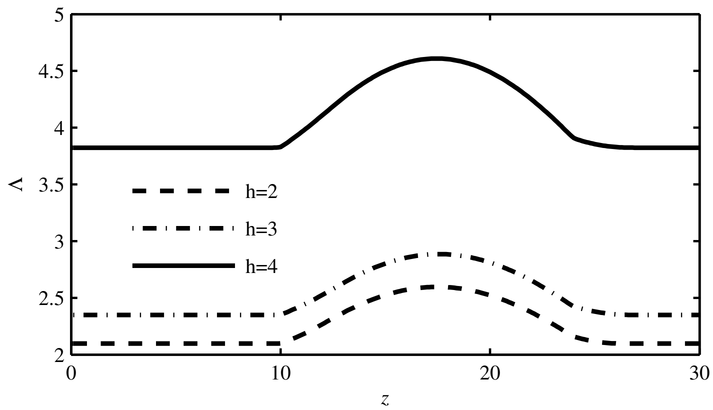

Figure 8: Distribution of the resistive impedance for different values of Hartmann number.

observed from this figure that the resistive impedance increases by the increase in the stenosis size. In addition, comparing the resistive impedance of elastic and rigid arteries indicates that the impedance of the elastic artery is more than the rigid artery.

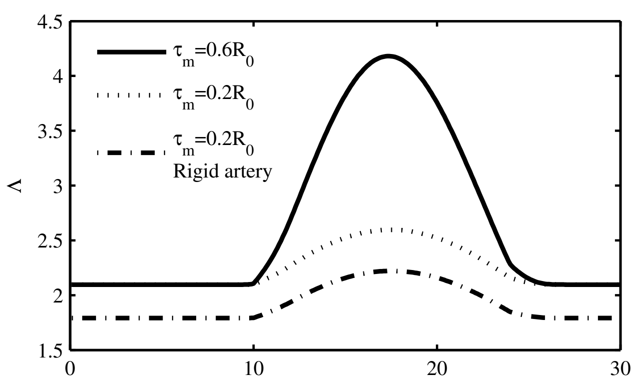

Figure 9: Distribution of the resistive impedance for different stenosis size.

Figure 10 depicts the three-dimensional resistive impedance along the axial direction z and time $t = 1$ for $\tau_m = 0.2R_0$. It is seen that unlike the rate of flow, the resistive impedance (Λ) increases by the increase of the time.

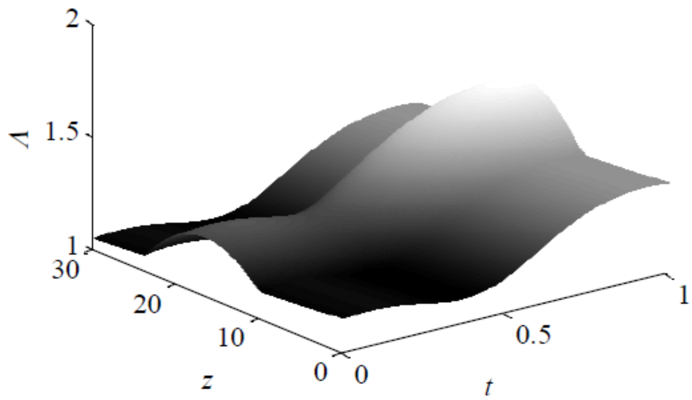

Figure 10: Surface plot of the resistive impedance.

5 Conclusion

The unsteady, laminar and two-dimensional flow of blood through a constriction artery is studied. Using Crank-Nicolson sheme, the discretized form of the governing nonlinear partial differential equations and the influences of the effective parameters on flow specifications such as the velocity profile, the rate of flow and the resistive to flow are examined. Our results demonstrate that the axial velocity and the rate of flow decreases by the increase in the stenosis size and also, the magnetic field has reduced effect on the blood fluid velocity. The resistive impedance decreases with the increase in the Hartmann number, so the action of a magnetic field, the volume of blood flow can be adjusted during surgeries. The blood flow characteristics among elastic artery is compared with the rigid ones and this difference between the axial velocity of the rigid and the elastic arteries shows the importance of the hypothesis of elastic blood vessels.

References

[1] A. Alshare, B. Tashtoush and H.H. El-Khalil, *Computational modelling of non-Newtonian blood flow through stenosed arteries in the presence of magnetic field*, J. Biomech. Eng. **135** (2013) 1–6.

[2] E. Belardinelli and S. Cavalcanti, *A new nonlinear two-dimensional model of blood motion in tapered and elastic vessels*, Comput. Bio. Medicine **21** (1991) 1–13.

[3] S. Chakravarty and P.K. Mandal, *Two-dimensional blood flow through tapered arteries under stenotic conditions*, Int. J. Nonlinear Mech. **35** (2000) 779–793.

[4] M. Deshpande, D. Giddens and F. Mabon, *Steady laminar flow through modelled vascular stenoses*, J. Biomech. **9** (1976) 165–174.

[5] A.R. Haghighi and M.A. Asl, *Mathematical modeling of micropolar fluid flow through an overlapping arterial stenosis*, Int. J. Biomath. **8** (2015) 1550056-1–1550056-15.

[6] A.R. Haghighi, M.A. Asl and K. Kiyasatfar, *Mathematical modeling of unsteady blood flow through elastic tapered artery with overlapping stenosed*, J. Brazilian Soc. Mech. Sci. Eng. **37** (2015) 571–578.

[7] A.R. Haghighi and M.A. Asl, *Numerical simulation of unsteady blood flow through an elastic artery with a non-symmetric stenisis*, Modares Mech. Engin. **14** (2014) 26–34.

[8] A.R. Haghighi, *Mathematical model of the impact of pressure drop on human body*, Selcuk J. Appl. Math. **13** (2012) 35–40.

[9] A.R. Haghighi, A.A. Kabdool, M.A. Asl and K. Kiyasatfar, *Numerical Investigation of Pulsatile Blood Flow in Stenosed Artery*, Int. J. Appl. Comput. Math. **2** (2016) 649–662.

[10] A.R. Haghighi and S. Asadi chalak, *Mathematical modelling of Sisko flow through a stenosed artery*, Int. J. Industrial Math. **14** (2017) 75–82.

[11] M. Ikbal, S. Chakravarty and P. Mandal, *Two-layered micropolar fluid flow through stenosed artery: effect of peripheral layer thickness*, Comput. Math. Appl. **58** (2009) 1328–1339.

[12] G. Liu, X. Wang, B. Ai and L. Liu, *Numerical study of pulsating flow through a tapered artery with stenosis*, Chinese J. Phys. **42** (2004) 401–409.

[13] P. Mandal, S. Chakravarty, A. Mandal and A. Amin, *Effect of body acceleration on unsteady pulsatile flow of non-Newtonian fluid through a stenosed artery*, Appl. Math. Comput. **189** (2007) 766–779.

[14] PF. Marques, MEC. Oliveira, AS. Franca and M. Pinotti, *Modeling and simulation of pulsatile blood flow with a physiologic wave pattern*, Appl. Math. Comput. **27** (2003) 458–478.

[15] Kh.S. Mekheimer, M.H. Haroun and M.A. Elkot, *Effects of magnetic field, porosity, and wall properties for anisotropically elastic multi-stenosis arteries on blood flow characteristics*, Appl. Math. Mech. **32** (2011) 1047–1064.

[16] K. Mekheimer and M. El Kot, *The micropolar fluid model for blood flow through a tapered arterywith a stenosis*, Acta. Mech. Sin. **189** (2008) 637–644.

[17] J.C. Misra, G.C. Shit, *Flow of a biomagnetic viscoelastic fluid in a channel with stretching walls*, J. Appl. Mech. **76** (2009) 061006-061006–9.

[18] J.C. Misra, G.C. Shit, S. Chandra and P.K. Kundu, *Hydromagnetic flow and heat transfer of a second-grade viscoelastic fluid in a channel with oscillatory stretching walls: application to the dynamics of blood flow*, J. Eng. Math. **69** (2011) 91–100.

[19] J.C. Misra, A. Sinha, G.C. Shit, *Mathematical modeling of blood flow in a porous vessel having double stenosis in the presence of an external magnetic field*, Int. J. Biomath. **4** (2011) 207–225.

[20] Z. Mortazavinia, A. Zare and A. Mehdizadeh, *Effects of renal artery stenosis on realistic model of abdominal aorta and renal arteries incorporating fluid-structure interaction and pulsatile non-Newtonian blood flow*, Appl. Math. Mech. **33** (2012) 165–176.

[21] S. Mukhopadhyay and G. Layek, *Numerical modeling of a stenosed artery using mathematical model of variable shape*, AAM Int. J. **3** (2008) 308–328.

[22] N. Mustapha, N. Amin, S. Chakravarty and P. Mandal, *Unsteady magnetohydrodynamic blood flow through irregular multi-stenosed arteries*, Comput. Bio. Med. **39** (2009) 896–906.

[23] R. Ponalagusamy and R. Tamil Selvi, *A study on two-layered model (Casson-Newtonian) for blood flow through an arterial stenosis: axially variable slip velocity at the wall*, J. Franklin Ins. **343** (2011) 2308–2321.

[24] P. Pontrelli, *Pulsatile blood flow in a pipe*, Comput. Fluids **27** (1998) 367–380.

[25] D. Sankar, *A two-fluid model for pulsatile flow in catheterized blood vessels*, Int. J. Nonlinear Mech. **44** (2009) 337–351.

[26] D. Sankar and U. Lee, *Mathematical modeling of pulsatile flow of non-Newtonian fluid in stenosed arteries*, Comm. Nonlinear Sci. Num. Simul. **7** (2009) 2971–2981.

[27] D. Sankar and U. Lee, *Nonlinear mathematical analysis for blood flow in a constricted artery under periodic body acceleration*, Commun. Nonlinear Sci. Numer. Simul. **16** (2011) 4390–4402.

[28] S. Shaw, P. Murthy and S. Pradhan, *The effect of body acceleration on two dimensional flow of Casson fluid through an artery with asymmetric stenosis*, Open Transp. Phenom. J. **2** (2010) 55-68.

[29] G.C. Shit, M. Roy, *Pulsatile flow and heat transfer of a magneto-micropolar fluid through a stenosed artery under the influence of body acceleration*, J. Mech. Med. Bio. **11** (2011) 643-661.

[30] G.C. Shit, *Computational modelling of blood flow development and its characteristics in magnetic environment*, Model. Simul. Eng. **2013** (2013) 1–12.

[31] G.C. Shit and S. Majee, *Pulsatile flow of blood and heat transfer with variable viscosity under magnetic and vibration environment*, J. Mag. Mag. Mat. **388** (2015) 106-115.

[32] S. Singh, *Numerical modeling of two-layered micropolar fluid through an normal and stenosed artery*, IJE-Transactions A: Basics **2** (2011) 177.

[33] V. Srivastava, R. Vishnoi, S. Mishra and P. Sinha, *A two-layered non-Newtonian arterial blood flowthrough an overlapping constriction*, AAM Int. J. **6** (2001) 41-57.